Check for updates

International Journal for Numerical Methods in Engineering

WILEY

RESEARCH ARTICLE OPEN ACCESS

Regularization in Structural Model Updating in the Presence of Noisy Data

Maria Girardi[1] | Cristina Padovani[1] | Daniele Pellegrini[1] | Leonardo Robol[1,2]

[1]Institute of Information Science and Technologies "A. Faedo" ISTI–CNR, Pisa, Italy | [2]Department of Mathematics, University of Pisa, Pisa, Italy

Correspondence: Daniele Pellegrini (daniele.pellegrini@isti.cnr.it)

Received: 26 November 2024 | **Revised:** 5 June 2025 | **Accepted:** 15 August 2025

Funding: This work was supported by the Italian National Research Council (REVOLUTION Project, Progetti di Ricerca @CNR, 2022–2025). The work of Leonardo Robol has been supported by the National Research Center in High Performance Computing, Big Data and Quantum Computing (CN1 – Spoke 6), by the Italian Ministry of University and Research awarded to the Department of Mathematics, University of Pisa, CUP I57G22000700001. These supports are gratefully acknowledged.

Keywords: engineering structures | model updating | nonlinear least squares problem | Tikhonov regularization | truncated singular value decomposition

ABSTRACT

This article addresses the presence of noise when solving the inverse problem of determining the material properties of an elastic engineering structure from measured vibration data. After identifying the frequencies, material properties are determined by solving an optimization problem. However, if the experimental frequencies are affected by noise (as often happens in practice), this can lead to inaccuracy due to the ill-conditioning of the problem. A regularization strategy based on Tikhonov regularization is discussed, and an automatic regularization parameter choice is introduced to deal with cases where the noise level is not known beforehand. The algorithm is tested on three examples, including artificial models where the exact solution is known and a case study from the Matilde donjon in Livorno, with experimental data measured by seismic stations during ambient vibration tests. The proposed method consistently performs well across all tests, validating the reliability of the approach.

1 | Introduction

Combining ambient vibration monitoring and finite element (FE) modeling through suitable model updating procedures allows us to estimate the boundary conditions and mechanical material properties of engineering structures made of linear elastic materials [1, 2]. Model updating is an inverse problem in which some experimental data measured on the structure are exploited to calibrate its numerical counterpart. Application of FE model updating to engineering structures and historical buildings involves the solution of a constrained minimum problem whose objective function is generally expressed as the discrepancy between experimental and numerical quantities, such as natural frequencies and mode shapes [3–8], which depend on unknown parameters, such as mechanical properties and mass densities of the constituent materials. Since the dependence of frequencies and mode shapes on the unknown parameters is nonlinear, model updating is a nonlinear least squares problem. The deterministic approach relying on calculating local or global minima of the above objective function is prone to the well-known drawbacks of inverse problems, like ill-posedness and ill-conditioning. The sensitivity of model updating to errors and uncertainties can undermine the robustness and reliability of the numerical procedures adopted for its solution.

Such inconveniences in inverse problems can be avoided by using regularization techniques like the Tikhonov regularization, mainly adopted for solving linear ill-posed problems [9–13]. Within this approach, the objective function is penalized by a term that incorporates prior information on the solution and

This is an open access article under the terms of the Creative Commons Attribution License, which permits use, distribution and reproduction in any medium, provided the original work is properly cited.

© 2025 The Author(s). *International Journal for Numerical Methods in Engineering* published by John Wiley & Sons Ltd.

depends on a regularization parameter that must be suitably determined. Applications of Tikhonov regularization to the nonlinear least squares problems typical of FE model updating are more recent and currently represent a challenging research topic [14–23].

The probabilistic approach based on Bayes' theorem offers an alternative to deterministic model updating [24–34]. In the Bayesian model updating, the unknown solution to the inverse problem is a random variable described using its distribution. Within this framework, the parameters' calibration involves maximizing the conditional probability of the parameters based on known random output measurements. The maximization is done by considering a prior probability distribution for the parameters, which reflects the engineer's judgement. Choosing these priors involves a subjective decision, which makes the Bayesian method similar to Tikhonov regularization in deterministic model updating [30]. Introducing an informative penalty term is equivalent to expressing an a priori belief about the solution and has a crucial role in the regularization approach.

In this article, particular attention has been devoted to the study and development of a robust method able to overcome the well-known drawbacks affecting inverse problems, like ill-posedness and the consequent possible significant changes in the output due to minimal input perturbation (the experimental frequencies and mode shapes). Adopting regularization techniques [12] to avoid misleading material properties identification and recover meaningful solutions has been investigated. Regularization is then applied to some simulated case studies, a criterion based on computing the Jacobian's Singular Value Decomposition (SVD) is considered, and the meaningfulness of solutions is examined.

The regularization techniques presented in this paper rely on an algorithm for the FE model updating based on the construction of the local parametric reduced-order models embedded in a trust-region scheme and implemented in NOSA-ITACA, a non-commercial FE code developed by the authors [35–37]. The algorithm [38–40] exploits the structure of the stiffness and mass matrices, and the fact that only a few of the smallest eigenvalues have to be calculated. The procedure enables the computation of eigenvalues and eigenvectors, thus solving the minimum problem very efficiently. Besides reducing the overall computation time of the numerical process and enabling the accurate analysis of large-scale models with little effort, the proposed algorithm allows for getting information on the solution's reliability and sensitivity to noisy experimental data [38].

The article is structured as follows. In Section 2, we recall the FE model updating problem, introduce the Tikhonov regularization [10–12], and discuss an efficient strategy for estimating the optimal regularization parameter λ. Section 3 analyzes two representative numerical examples and a real case study, the Matilde donjon in the Old Fortress in Livorno, Italy. We demonstrate that when noise pollutes the measured data, the estimated values of material properties may be meaningless, and a proper choice of a regularization parameter λ in a Tikhonov-based approach can cure this problem. Moreover, we show that the strategy proposed in Section 2 for choosing the regularization parameter provides excellent results and improves reliability for the model updating scheme under consideration.

2 | Deterministic Model Updating and Tikhonov Regularization

Using experimental modal properties of a structure makes it possible to calibrate its FE model via model updating procedures. The goal of FE model updating is to determine the unknown characteristics of a structure, such as materials' properties and boundary conditions, by matching experimental and numerical frequencies and mode shapes [2].

The model updating problem can be formulated as an optimization problem by assuming that the stiffness $\mathbf{K}(\mathbf{x})$ and mass $\mathbf{M}(\mathbf{x})$ matrices of the FE model depend on a parameter vector $\mathbf{x}$ belonging to the box $\Omega \subset \mathbb{R}^p$. Solving the generalized eigenvalue problem

$$\mathbf{K}(\mathbf{x})\,\mathbf{v}(\mathbf{x}) = \omega^2(\mathbf{x})\,\mathbf{M}(\mathbf{x})\,\mathbf{v}(\mathbf{x}) \tag{1}$$

allows us to calculate the frequencies $f_1^M(\mathbf{x}) = \omega_1(\mathbf{x})/2\pi$, $\ldots$, $f_q^M(\mathbf{x}) = \omega_q(\mathbf{x})/2\pi$ and the corresponding eigenvectors $\mathbf{v}_1^M(\mathbf{x})$, $\ldots$, $\mathbf{v}_q^M(\mathbf{x})$. To calibrate the FE model, we have to determine the optimal value of $\mathbf{x} \in \Omega$ that minimizes the function

$$\phi(\mathbf{x}) = \sum_{i=1}^{q} w_i^2 [f_i - f_i^M(\mathbf{x})]^2 \tag{2}$$

which measures the distance between the experimental frequencies f_i and the numerical counterparts $f_i^M(\mathbf{x})$. Scalars w_i are the weights that should be given to each frequency in the optimization scheme (usually, $w_i = 1$ or $w_i = f_i^{-1}$, for $i = 1, \ldots, q$).

The minimum problem we must solve is a nonlinear least squares problem, and the numerical procedure implemented in the NOSA-ITACA code to minimize the function ϕ is based on a trust region scheme [39, 40]. By modifying the Lanczos' projection scheme used to compute the first (smallest) eigenvalues (and corresponding eigenvectors), we obtain local parametric reduced-order models that, embedded in the trust-region scheme, are the basis for an efficient algorithm that minimizes the objective function ϕ in Ω.

As an inverse problem, model updating is affected by drawbacks like ill-posedness and possible significant changes in the optimal parameters due to minimal perturbation of the experimental frequencies. We then investigate regularization techniques, including Tikhonov's approach, to avoid the well-known inconveniences characterizing inverse problems.

The following subsection recalls the Tikhonov regularization for linear and nonlinear least squares problems [11]. The application to the nonlinear least squares problem arising from minimizing the objective function (2) in Ω is dealt with in Section 2.2; criteria for selecting the regularization parameter are discussed in Section 2.3.

10970207, 2025, 17, Downloaded from https://onlinelibrary.wiley.com/doi/10.1002/nme.70113 by CNR Pisa, Wiley Online Library on [04/09/2025]. See the Terms and Conditions (https://onlinelibrary.wiley.com/terms-and-conditions) on Wiley Online Library for rules of use; OA articles are governed by the applicable Creative Commons License

2.1 | Tikhonov Regularization for the Linear and Nonlinear Least Squares Problems: General Results

Let us consider the linear least squares problem

$$\min_{\mathbf{y}\in\mathbb{R}^n} \|\mathbf{A}\mathbf{y} - \mathbf{b}'\|_2^2 \tag{3}$$

where $\|\cdot\|_2$ denotes the Euclidean norm, $\mathbf{A}$ is a full-rank $m \times n$ real matrix with $m \geq n$, and $\mathbf{b}' \in \mathbb{R}^m$ is the data vector affected by an unknown error $\boldsymbol{\delta}\mathbf{b}$,

$$\mathbf{b}' = \mathbf{b} + \delta b \tag{4}$$

with $\mathbf{b}$ the error-free part of $\mathbf{b}'$.

The solution to problem (3) satisfies the normal equations $\mathbf{A}^T\mathbf{A}\mathbf{y} = \mathbf{A}^T\mathbf{b}'$ and is

$$\mathbf{y}' = (\mathbf{A}^T\mathbf{A})^{-1}\mathbf{A}^T\mathbf{b}' = \mathbf{y}^b + (\mathbf{A}^T\mathbf{A})^{-1}\mathbf{A}^T\boldsymbol{\delta}\mathbf{b} \tag{5}$$

with $\mathbf{y}^b$ the solution corresponding to the error-free vector $\mathbf{b}$. When $\mathbf{A}^T\mathbf{A}$ is ill-conditioned, its inverse can have a huge norm and therefore cause an undesired amplification of the input noise $\boldsymbol{\delta}\mathbf{b}$. Therefore, to determine an approximation of $\mathbf{y}^b$, instead of (3), it is preferred to consider the penalized problem

$$\min_{\mathbf{y}\in\mathbb{R}^n}\left[\|\mathbf{A}\mathbf{y} - \mathbf{b}'\|_2^2 + \lambda^2\|\mathbf{y}\|_2^2\right] \tag{6}$$

with $\lambda \in \mathbb{R}$ and solve the shifted normal equation $(\mathbf{A}^T\mathbf{A} + \lambda^2\mathbf{I}_n)\mathbf{y} = \mathbf{A}^T\mathbf{b}'$, whose solution is

$$\mathbf{y}'_\lambda = (\mathbf{A}^T\mathbf{A} + \lambda^2\mathbf{I}_n)^{-1}\mathbf{A}^T\mathbf{b}' = \mathbf{y}^b_\lambda + (\mathbf{A}^T\mathbf{A} + \lambda^2\mathbf{I}_n)^{-1}\mathbf{A}^T\boldsymbol{\delta}\mathbf{b} \tag{7}$$

with $\mathbf{y}^b_\lambda$ the solution corresponding to $\mathbf{b}$ and $\mathbf{I}_n$ the $n \times n$ identity matrix. Penalizing problem (3) and then shifting the matrix $\mathbf{A}^T\mathbf{A}$ with the parameter λ^2 can be interpreted as applying a low-pass filter to the singular values of $\mathbf{A}$ that mitigates their effect on amplifying the noise $\boldsymbol{\delta}\mathbf{b}$. Indeed, let

$$\mathbf{A} = \mathbf{U}\boldsymbol{\Sigma}\mathbf{V}^T = \sum_{j=1}^{n}\sigma_j\mathbf{u}_j\mathbf{v}_j^T \tag{8}$$

be the singular value decomposition (SVD) of $\mathbf{A}$, and assume for simplicity that $m = n$ and $\mathbf{A}$ is symmetric, then we have

$$\mathbf{y}' - \mathbf{y}^b = \sum_{j=1}^{n}\mathbf{v}_j\frac{\mathbf{u}_j^T\boldsymbol{\delta}\mathbf{b}}{\sigma_j}, \qquad \mathbf{y}'_\lambda - \mathbf{y}^b_\lambda = \sum_{j=1}^{n}\mathbf{v}_j\frac{\sigma_j^2}{\sigma_j^2+\lambda^2}\frac{\mathbf{u}_j^T\boldsymbol{\delta}\mathbf{b}}{\sigma_j} \tag{9}$$

The quantity $\frac{\sigma_j^2}{\sigma_j^2+\lambda^2}$ introduced in Equation (9) and called Tikhonov filter factor is close to 1 for $\sigma_j \gg \lambda$ and well-approximated by $\frac{\sigma_j^2}{\lambda^2}$ for $\sigma_j \ll \lambda$. Hence, for singular values $\sigma_j \gg \lambda$ the filter factor has almost no effect on that part of the solution. On the other hand, if $\sigma_j \ll \lambda$ the filter factor is small and damps the amplification effect of σ_j^{-1}, replacing it with a milder λ^{-1}.

We remark that passing to normal equations and considering $\mathbf{A}^T\mathbf{A}$ in place of $\mathbf{A}$ is usually not recommendable from the perspective of numerical stability since the conditioning of the problem is squared, and the amplification of the perturbations is generally much more severe. Hence, although we discuss normal equations for theoretical reasons, our implementation will be based on the SVD, which is mathematically equivalent but does not present this issue.

Let us now assume that the components $\delta b_i, i = 1, \ldots, m$ of $\boldsymbol{\delta}\mathbf{b}$ are independent, normally distributed random variables with zero mean and variance σ^2 [41]. Then $\boldsymbol{\delta}\mathbf{b}$ is a random vector with zero mean and covariance matrix $\sigma^2\mathbf{I}_m$

$$\mathbb{E}[\boldsymbol{\delta}\mathbf{b}] = \mathbf{0}, \qquad \mathbb{E}[\boldsymbol{\delta}\mathbf{b}\boldsymbol{\delta}\mathbf{b}^T] = \sigma^2\mathbf{I}_m \tag{10}$$

From Equation (7), we get that $\mathbf{y}'_\lambda - \mathbf{y}^b_\lambda$ is also a random vector with zero mean and covariance matrix

$$\begin{aligned}&\mathbb{E}[(\mathbf{y}'_\lambda - \mathbf{y}^b_\lambda)(\mathbf{y}'_\lambda - \mathbf{y}^b_\lambda)^T]\\ &= \sigma^2(\mathbf{A}^T\mathbf{A} + \lambda^2\mathbf{I}_n)^{-1}\mathbf{A}^T\mathbf{A}(\mathbf{A}^T\mathbf{A} + \lambda^2\mathbf{I}_n)^{-1}\\ &= \sum_{j=1}^{n}\frac{\sigma^2\sigma_j^2}{(\lambda^2+\sigma_j^2)^2}\mathbf{v}_\mathbf{j}\mathbf{v}_\mathbf{j}^T \prec \frac{\sigma^2}{\lambda^2}\mathbf{I}_n\end{aligned} \tag{11}$$

where $\prec$ denotes the ordering over positive definite matrices [42]; as a consequence, the spectral norm of the covariance matrix is bounded by σ^2/λ^2. Choosing λ larger than the variance of the noise yields an error $\mathbf{y}'_\lambda - \mathbf{y}^b_\lambda$ concentrated around its (zero) mean.

A similar argument carries over to more general nonlinear least squares problems if they are sufficiently smooth around the minimum point. Consider the nonlinear least squares problem

$$\min_{\mathbf{y}\in\mathbb{R}^n} \|\mathbf{h}(\mathbf{y}) - \mathbf{b}'\|_2^2 \tag{12}$$

with $\mathbf{b}'$ in Equation (4) and $\mathbf{h}$ a nonlinear vector function. We denote by $\mathbf{y}^b$ the solution corresponding to the error-free vector $\mathbf{b}$, then $\mathbf{y}^b$ satisfies the necessary optimality condition

$$D\mathbf{h}(\mathbf{y}^b)^T(\mathbf{h}(\mathbf{y}^b) - \mathbf{b}) = \mathbf{0} \tag{13}$$

where $D\mathbf{h}$ denotes the Jacobian of $\mathbf{h}$.

For a small perturbation $\boldsymbol{\delta}\mathbf{b}$ we can estimate the corresponding optimum by using the expansion

$$\mathbf{h}(\mathbf{y}) = \mathbf{h}(\mathbf{y}^b) + D\mathbf{h}(\mathbf{y}^b)(\mathbf{y} - \mathbf{y}^b) + O(\|\mathbf{y} - \mathbf{y}^b\|_2^2) \tag{14}$$

Using the above affine approximation for $\mathbf{h}(\mathbf{y})$ and writing the necessary minimality conditions, one retrieves the Gauss–Newton method, and we can use one step as an estimate for the modified solution $\mathbf{y}'$ as follows:

$$\mathbf{y}' \approx \mathbf{y}^b + \left[D\mathbf{h}(\mathbf{y}^b)^T D\mathbf{h}(\mathbf{y}^b)\right]^{-1} D\mathbf{h}(\mathbf{y}^b)^T\boldsymbol{\delta}\mathbf{b} \tag{15}$$

where we have used the optimality condition (13), and dropped second-order terms.

The formula (15) retains the same structure of the normal equations for the linear case, with the Jacobian $D\mathbf{h}(\mathbf{y}^b)$ in place of the matrix $\mathbf{A}$, which is not surprising since they have been obtained by locally linearizing the objective function. This allows

10970207, 2025, 17, Downloaded from https://onlinelibrary.wiley.com/doi/10.1002/nme.70113 by CNR Pisa, Wiley Online Library on [04/09/2025]. See the Terms and Conditions (https://onlinelibrary.wiley.com/terms-and-conditions) on Wiley Online Library for rules of use; OA articles are governed by the applicable Creative Commons License

us to recover the filtering interpretation of the Tikhonov regularization by writing

$$\mathbf{y}' - \mathbf{y}^b \approx \sum_{j=1}^{n} \mathbf{v}_j \frac{\mathbf{u}_j^T \boldsymbol{\delta}\mathbf{b}}{\sigma_j}, \qquad D\mathbf{h}(\mathbf{y}^b) = \sum_{j=1}^{n} \sigma_j \mathbf{u}_j \mathbf{v}_j^T \tag{16}$$

where the right formula indicates the SVD of the Jacobian at $\mathbf{y}^b$.

Adding a penalty term in Equation (12) leads to the following approximation

$$\mathbf{y}'_\lambda - \mathbf{y}^b_\lambda \approx \sum_{j=1}^{n} \mathbf{v}_j \frac{\sigma_j^2}{\sigma_j^2 + \lambda^2} \frac{\mathbf{u}_j^T \boldsymbol{\delta}\mathbf{b}}{\sigma_j} \tag{17}$$

analogous to $(9)_2$. Hence, up to higher-order terms, we recover exactly the upper bound of (11).

The next section shows the application of the Tikhonov approach to the nonlinear least squares problem arising in the model updating of linear elastic structures.

2.2 | Tikhonov Regularization for FE Model Updating

This section aims to show that a regularization strategy can be beneficial in the presence of noisy frequencies.

Assuming that the experimental frequencies vector $\mathbf{f} = (f_1, \ldots, f_q)^T$ is contaminated with a noise $\boldsymbol{\delta}\mathbf{f}$, setting $\mathbf{f}' = \mathbf{f} + \boldsymbol{\delta}\mathbf{f}$ and $\Phi(\mathbf{x}) = (f_1^M(\mathbf{x}), \ldots, f_q^M(\mathbf{x}))^T$, the model updating problem consists in finding a minimizer to the objective function

$$F(\mathbf{x}) = \|\Phi(\mathbf{x}) - \mathbf{f}'\|_2^2 \tag{18}$$

This function, obtained from Equation (2) setting $w_i = 1$ and replacing $\mathbf{f}$ with $\mathbf{f}'$, is smooth everywhere with the only possible exception of points where frequencies become multiple, when only continuity is preserved. Smoothness enables the development of efficient methods, like the one proposed by the authors, based on a trust-region approach tuned for the case of structural analysis and presented in [38, 39].

The ideal situation would be to have $\boldsymbol{\delta}\mathbf{f} = \mathbf{0}$, so the solution of the optimization problem coincides with the actual parameters. However, real-world measurements are subject to noise and uncertainties, so we need to deal with the fact that $\mathbf{f}$ is affected by an error $\boldsymbol{\delta}\mathbf{f}$.

We have stressed that the addition of $\boldsymbol{\delta}\mathbf{f}$ can be "amplified" by the solution of the inverse problem. It is possible to mitigate this error amplification by adding a penalty term to the objective function, using a Tikhonov approach

$$F_\lambda(\mathbf{x}) = F(\mathbf{x}) + \lambda^2 \|\mathbf{x} - \hat{\mathbf{x}}\|_2^2 \tag{19}$$

where $\lambda \geq 0$ is the Tikhonov parameter and $\hat{\mathbf{x}}$ is chosen as an initial estimate for unknown material properties. We can note that two extreme cases can occur:

1. If $\lambda = 0$, then (19) reduces to the original optimization problem (18). Hence, we expect it not to be robust against noise.
2. If λ is large, say in the limit for $\lambda \to \infty$, then the term $F(\mathbf{x})$ becomes negligible, and the minimum of $F_\lambda(\mathbf{x})$ will be $\hat{\mathbf{x}}$, completely ignoring the values of the frequencies.

Clearly, both these behaviors are undesirable. However, there exists a "trade-off" choice of the parameter λ such that the noise is filtered effectively, but at the same time, the solution computed is not biased to be close to $\hat{\mathbf{x}}$. We will later refer to this value of λ as the optimal regularization parameter for the problem under consideration.

Whenever the standard deviation of the noise is known, the parameter can be chosen using the Discrepancy Principle [43, 44]; if computing the SVD is feasible, one can choose λ of the same order as the smallest singular values of interest [14, 45]. Several other techniques are available for large-scale problems, such as the Generalized Cross Validation (GCV) method [14, 45–48], the L-curve method [14, 49–51]. These will not be of interest in our context, where the number of parameters is small, and computing the SVD of the Jacobian is always feasible.

The algorithm presented in the [38, 39] has been suitably modified to solve the optimization problem given by $F_\lambda(\mathbf{x})$ instead of $F(\mathbf{x})$. The algorithm has been tested on the two simple yet meaningful examples described in Section 3, where this optimal regularization parameter can be immediately recognized. In particular, the numerical procedure has been used to compute the solutions in problems where the exact solution is known explicitly, under the effect of noise, with different regularization parameters.

2.3 | Automatic Selection of the Regularization Parameter

Consider the regularized objective function $F_\lambda(\mathbf{x})$ defined in Equation (19). Note that $\mathbf{x}'_\lambda$ minimizes $F_\lambda(\mathbf{x})$ if and only if $\mathbf{x}'_\lambda$ minimizes the function $T_\lambda(\mathbf{x})$, with

$$T_\lambda(\mathbf{x}) = \|\Phi_\lambda(\mathbf{x}) - \mathbf{f}'_\lambda\|_2^2 \tag{20}$$

where

$$\Phi_\lambda(\mathbf{x}) = \begin{bmatrix} \Phi(\mathbf{x}) \\ \lambda \mathbf{x} \end{bmatrix}, \qquad \mathbf{f}'_\lambda = \mathbf{f}_\lambda + \begin{bmatrix} \boldsymbol{\delta}\mathbf{f} \\ \mathbf{0} \end{bmatrix}, \quad \mathbf{f}_\lambda = \begin{bmatrix} \mathbf{f} \\ \lambda \hat{\mathbf{x}} \end{bmatrix} \tag{21}$$

From Equation $(21)_1$, we get

$$D\Phi_\lambda(\mathbf{x}^f_\lambda) = \begin{bmatrix} D\Phi(\mathbf{x}^f_\lambda) \\ \lambda \mathbf{I}_p \end{bmatrix} \tag{22}$$

and then

$$D\Phi_\lambda(\mathbf{x}^f_\lambda)^T D\Phi_\lambda(\mathbf{x}^f_\lambda) = D\Phi(\mathbf{x}^f_\lambda)^T D\Phi(\mathbf{x}^f_\lambda) + \lambda^2 \mathbf{I}_p \tag{23}$$

10970207, 2025, 17, Downloaded from https://onlinelibrary.wiley.com/doi/10.1002/nme.70113 by CNR Pisa, Wiley Online Library on [04/09/2025]. See the Terms and Conditions (https://onlinelibrary.wiley.com/terms-and-conditions) on Wiley Online Library for rules of use; OA articles are governed by the applicable Creative Commons License

with $\mathbf{x}_\lambda^f$ the solution corresponding to $\mathbf{f}_\lambda$. Therefore, using $D\Phi_\lambda$ in place of $D\mathbf{h}$ in Equation (16) yields again the filtering interpretation

$$\mathbf{x}'_\lambda - \mathbf{x}_\lambda^f \approx \sum_{j=1}^{n} \mathbf{v}_j \frac{\sigma_j^2}{\sigma_j^2 + \lambda^2} \frac{\mathbf{u}_j^T \delta\mathbf{f}}{\sigma_j} \tag{24}$$

This result can guide our selection of the regularization parameter λ. If a priori information on the noise level is available, then taking $\lambda \approx \sigma_1 \frac{\|\delta\mathbf{f}\|}{\|\mathbf{f}\|}$ is a good choice. This controls the error terms from the above equation without deviating too much from the original problem and is based on the discrepancy principle already mentioned before [43, 44]. However, when this information is not available, we can still devise an effective strategy by introducing automatic parameter regularization.

In view of (24), we have to choose λ slightly larger than the smallest singular value to smooth the noise in the low frequencies. In our implementation, this has been done by the following heuristic:

$$\lambda = \tau \max\left\{10^{-3}\sigma_{\max}(D\Phi(\mathbf{x})), \sigma_{\min}(D\Phi(\mathbf{x}))\right\} \tag{25}$$

for an approriate $\tau > 1$. If τ is large, then the solution will be altered by the regularization process, but the method will be able to withstand a larger level of noise. For the case studies examined in this paper, the value $\tau = 1.2$ has been verified to be reasonably reliable. The scalar 10^{-3} is a safeguard to avoid choosing a parameter that is too small and unable to filter realistic noise levels in case of singular (or close to singular) Jacobians. Note that this is not a particularly aggressive filtering: Higher values for λ might be preferable for more significant noise levels.

A different strategy might enable the development of an even more robust method for high-noise settings. In particular, it can be beneficial to incorporate knowledge about the noise level if it is available.

As we see in the numerical experiments, this conservative choice can provide a beneficial effect.

This choice is made in the spirit of the *truncated SVD*, or TSVD, often used in regularization problems [10], and has been embedded in the trust-region solver based on Lanczos projections developed in [38, 39].

Note that the regularization parameter defined in this way depends on the point $\mathbf{x}$.

In addition, one may draw a connection between this approach and the Levenberg–Marquardt method [52, 53], obtained by regularizing the Jacobian during the Gauss–Newton steps. Nevertheless, we stress a fundamental difference between these two approaches. In the Levenberg–Marquardt method, the regularization is meant to improve the convergence behavior, both in speed and robustness, but the optimization problem is left unchanged, and it is desired that the parameter λ disappears at the end of the process. In our approach, we aim to modify the optimization problem and look for the minimum of a modified problem, which is less subject to noise. A comparison between the two approaches is provided in Section 3.

Concerning the choice of λ, we have verified that modifying its value at every regeneration of the model in the trust region solver leads to poor convergence properties: The fact that the underlying optimization problem is changed while the method is running leads to oscillation close to the solution. This kind of choice is sometimes referred to as non-stationary Tikhonov regularization. Therefore, we have devised a relaxation strategy that works as follows. At every step, a new parameter $\lambda^{(\text{new})}$ is chosen according to the TSVD criterion; then, we set $\lambda = \gamma\lambda^{(\text{new})} + (1-\gamma)\lambda^{(\text{old})}$, where $\lambda^{(\text{old})}$ is the parameter used in the previous step. The parameter γ has been chosen as 0.15, as this has been verified to provide good performance.

Finally, to make the strategy reliable and robust, we note that in the optimization problems under consideration, the magnitude of the parameters is highly non-homogeneous. For instance, Young's moduli are usually in the interval $[10^8, 10^{10}]$ (if measured in Pa), whereas mass densities range in $[10^2, 10^4]$ (if measured in $\frac{\text{kg}}{\text{m}^3}$). Therefore, it does not make sense to consider perturbations in absolute value because their effect might differ significantly depending on the parameter they are affecting. To take this effect into account, we perform a local analysis of the scaled problem

$$G(\mathbf{z}) = \|\Phi(\mathbf{D}\mathbf{z}) - \mathbf{f}'\|_{\mathbf{w},2}^2, \quad \mathbf{z} = \mathbf{D}^{-1}\mathbf{x}, \quad \|\mathbf{s}\|_{\mathbf{w},2} = \sqrt{\mathbf{s}^T\mathbf{D}_\mathbf{w}^2\mathbf{s}} \tag{26}$$

where $\mathbf{D}$ is a diagonal matrix with the magnitude of the entries in the vectors $\mathbf{x}$ on the diagonal and $\mathbf{D}_\mathbf{w} = \text{diag}(w_1, \ldots, w_q)$, with w_i the weights introduced in Equation (2). Thus, the parameter vector is always close to the vector of all ones, and relative perturbations to the parameters are measured. The scaling matrix $\mathbf{D}_\mathbf{w}$ is employed to consider different weights given to the frequencies in the optimization problem. The choice of the diagonal matrices with the weights to guarantee relative accuracy on the frequencies is discussed in more detail in [39].

3 | Numerical Experiments and a Real Case Study

The algorithm described in the previous section was implemented in MATLAB R2022b and integrated into the finite element code NOSA-ITACA. In this section, we validate the proposed regularization approach by analyzing two numerical examples and a real case study. All results were obtained on an Intel Core i7-9700K PC running at 3.60 GHz x 8 with 16 GB of RAM, 64-bit. We introduce some notations used in the following subsections. We denote by $\mathbf{x}_0^f$ a minimum point of the objective function (18) (no regularization) in the absence of noise. For a fixed noise level δ, we replace the frequencies f_i with the perturbed ones

$$f_i' = f_i(1 + (2\ \texttt{rand} - 1)\delta), \quad i = 1, \ldots, q \tag{27}$$

with `rand` the Matlab function returning a random scalar drawn from the uniform distribution in the interval (0,1). Given the regularization parameter λ and the initial estimate $\hat{\mathbf{x}}$, we denote by $\mathbf{x}'_\lambda$ a solution of (19) calculated by using the noisy data f_i' and

10970207, 2025, 17, Downloaded from https://onlinelibrary.wiley.com/doi/10.1002/nme.70113 by CNR Pisa, Wiley Online Library on [04/09/2025]. See the Terms and Conditions (https://onlinelibrary.wiley.com/terms-and-conditions) on Wiley Online Library for rules of use; OA articles are governed by the applicable Creative Commons License

consider the maximum relative errors ϵ_λ (depending on δ) and $\hat{\epsilon}$ defined as

$$\epsilon_\lambda = \max_{i=1,\dots,p} \frac{|x'_{\lambda i} - x^f_{0i}|}{x^f_{0i}} \tag{28}$$

$$\hat{\epsilon} = \max_{i=1,\dots,p} \frac{|\hat{x}_i - x^f_{0i}|}{x^f_{0i}} \tag{29}$$

To analyze the results of the automatic selection procedure described in Section 2, for each noise level δ, we calculate the maximum relative error ϵ_δ as follows. For δ fixed, we run 100 analyses using the perturbed frequencies defined in Equation (27). For each analysis, the optimal value of λ is chosen according to the selection procedure described above, and the corresponding solution $\mathbf{x}'_\lambda$ and maximum relative error ϵ_λ defined in Equation (28) are calculated. The maximum relative error ϵ_δ is defined as the maximum of the quantities ϵ_λ over the 100 optimal values of λ in the regularized case, and as the maximum of the quantities ϵ_0 over the 100 runs in the case without regularization. In all the examples described below, the starting point of the iterative process characterizing the trust-region scheme [39] coincides with the initial estimate $\hat{\mathbf{x}}$.

3.1 | Arch on Piers

Consider the arch on piers sketched in Figure 1, modeled via NOSA-ITACA using 336 plane strain 4-node quadrilateral elements [36]. We assume that the structure clamped at the base is made of the three different materials shown in Figure 1, constituting the arch and the pillars, whose Young's moduli, mass densities, and Poisson's ratios are

$$E^e_1 = 3.250 \text{ GPa}, \quad E^e_2 = 5.0 \text{ GPa} \quad E^e_3 = 4.800 \text{ GPa} \tag{30}$$

$$\rho^e_1 = 1800 \ \frac{\text{kg}}{\text{m}^3}, \quad \rho^e_2 = 2200 \ \frac{\text{kg}}{\text{m}^3} \quad \rho^e_3 = 2100 \ \frac{\text{kg}}{\text{m}^3} \tag{31}$$

$$\nu^e_1 = 0.2, \quad \nu^e_2 = 0.2 \quad \nu^e_3 = 0.1 \tag{32}$$

We calculate the structure's first five frequencies f_i (expressed in Hz) using the material properties assigned above

$$\mathbf{f} = (9.58, 14.87, 23.17, 39.17, 62.84)^T \tag{33}$$

and we fix the mechanical characteristics of material 1 (the arch). Then, for a fixed noise level δ, we consider the perturbed frequencies f'_i, $i = 1, \dots, 5$ defined in Equation (27) and for $\mathbf{x} = (E_2, \rho_2, E_3, \rho_3)^T$, we calculate the minimum of (19) in the box Ω defined by the following inequalities

$$1.0 \le E_2, E_3 \le 9.0, \quad 10^3 \le \rho_2, \rho_3 \le 3.0 \times 10^3 \tag{34}$$

We choose as initial estimate $\hat{\mathbf{x}}$ the midpoint of Ω,

$$\hat{\mathbf{x}} = (5.0, 2.0 \times 10^3, 5.0, 2.0 \times 10^3)^T \tag{35}$$

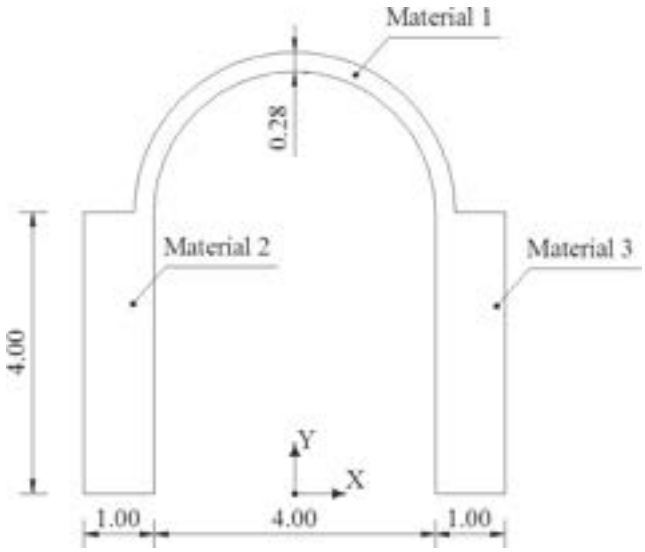

FIGURE 1 | The arch on piers (lengths in meters).

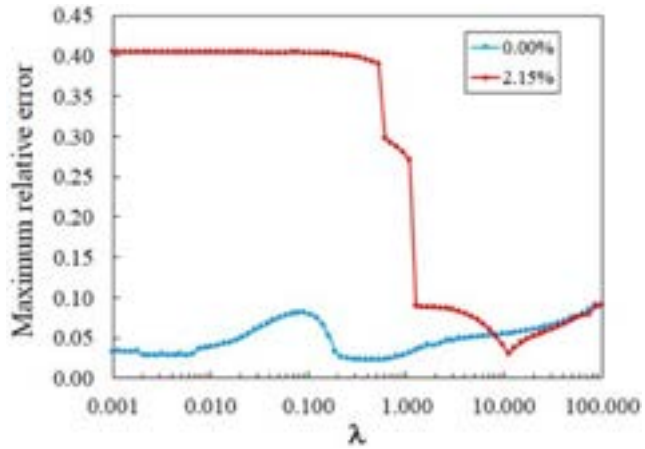

FIGURE 2 | Arch on piers – Maximum relative error ϵ_λ for different noise levels δ vs. the regularization parameter λ and initial estimate $\hat{\mathbf{x}} = (5.0, 2.0 \times 10^3, 5.0, 2.0 \times 10^3)^T$.

(the units have been omitted for notation convenience), thus the maximum relative error of $\hat{\mathbf{x}}$ defined in Equation (29) is $\hat{\epsilon} = 10\%$, with

$$\mathbf{x}^f_0 = (E^e_2, \rho^e_2, E^e_3, \rho^e_3)^T = (5.0, 2.2 \times 10^3, 4.8, 2.1 \times 10^3)^T \tag{36}$$

Figure 2 reports the value of the maximum relative error ϵ_λ defined in Equation (28) as a function of λ, for $\delta = 0.0\%$ and $\delta = 2.15\%$.

We note that as the regularization parameter λ grows, the difference of the errors ϵ_λ for the two noise levels disappears, as expected: The solution converges to the chosen $\hat{\mathbf{x}}$, and therefore the maximum relative error converges to 10%. On the other hand, when no regularization is used, the case with noise has a much higher error, greater than 40%. When using a good choice of the regularization parameter, it is possible to take the error down to less than 5%.

10970207, 2025, 17, Downloaded from https://onlinelibrary.wiley.com/doi/10.1002/nme.70113 by CNR Pisa, Wiley Online Library on [04/09/2025]. See the Terms and Conditions (https://onlinelibrary.wiley.com/terms-and-conditions) on Wiley Online Library for rules of use; OA articles are governed by the applicable Creative Commons License

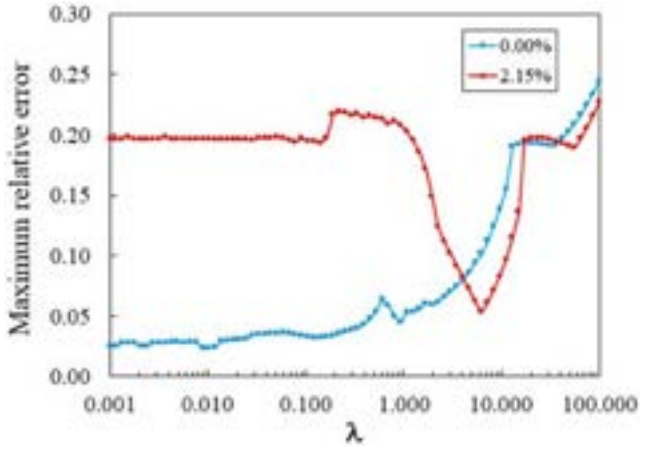

FIGURE 3 | Arch on piers – Maximum relative error ϵ_λ for different noise levels δ vs. the regularization parameter λ and initial estimate $\hat{\mathbf{x}} = (6.75, 2.25 \times 10^3, 6.75, 2.25 \times 10^3)^T$.

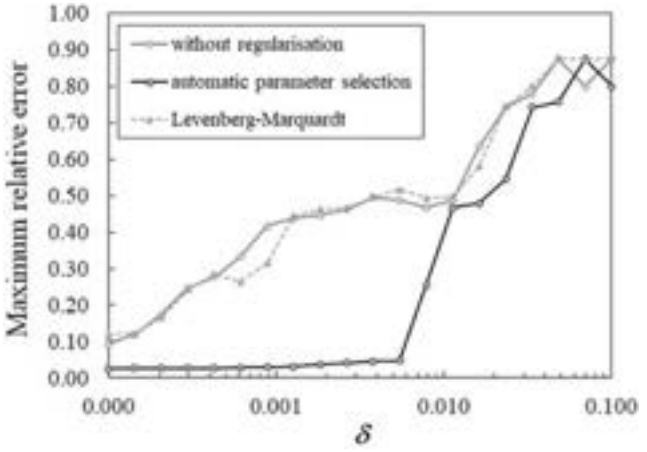

FIGURE 4 | Arch on piers – Maximum relative error ϵ_δ vs. the noise δ; comparison between the unregularized method, the Levenberg–Marquardt method and the automatic parameter selection with initial estimate $\hat{\mathbf{x}} = (5.0, 2.0 \times 10^3, 5.0, 2.0 \times 10^3)^T$.

With reference to Figure 2, for $\delta = 2.15\%$, the optimal value of the regularization parameter is $\lambda = 11.24$ and the minimum point of the objective function (19) is

$$\mathbf{x}'_\lambda = (4.93, 2.14 \times 10^3, 4.95, 2.14 \times 10^3)^T \tag{37}$$

with a maximum relative error $\epsilon_\lambda = 3.04\%$.

Figure 3 reports the value of the maximum relative error ϵ_λ as a function of λ, for another choice of the initial estimate

$$\hat{\mathbf{x}} = (6.75, 2.25 \times 10^3, 6.75, 2.25 \times 10^3)^T \tag{38}$$

In this case, the maximum relative error $\hat{\epsilon}$ is about 25%. For this choice of $\hat{\mathbf{x}}$ and for $\delta = 2.15\%$, the optimal value of the regularization parameter is $\lambda = 6.27$ and the minimum point is

$$\mathbf{x}'_\lambda = (4.96, 2.09 \times 10^3, 4.66, 2.21 \times 10^3)^T \tag{39}$$

with a maximum relative error $\epsilon_\lambda = 5.32\%$.

The results of the automatic selection procedure described in Section 2 are reported in Figure 4, which plots the maximum relative error ϵ_δ defined at the beginning of this Section, as a function of the noise level δ, with (black line) and without (grey line) regularization.

The beneficial effect of the regularization is evident: For noise levels less than 0.6%, ϵ_δ is about 4.7%, whereas, without regularization, ϵ_δ reaches 50%.

We note that, for high levels of noise, regularization yields results on par with the standard approach, and is not particularly beneficial. This is consistent with the typical behavior of Tikhonov regularizations [49]: A larger regularization parameter is required for higher noise levels, and while this effectively mitigates the noise, it also visibly modifies the recovered solution.

To assess the effectiveness of the proposed method, we compared it with the standard Levenberg–Marquardt implementation available in MATLAB (the `lsqnonlin` function). In

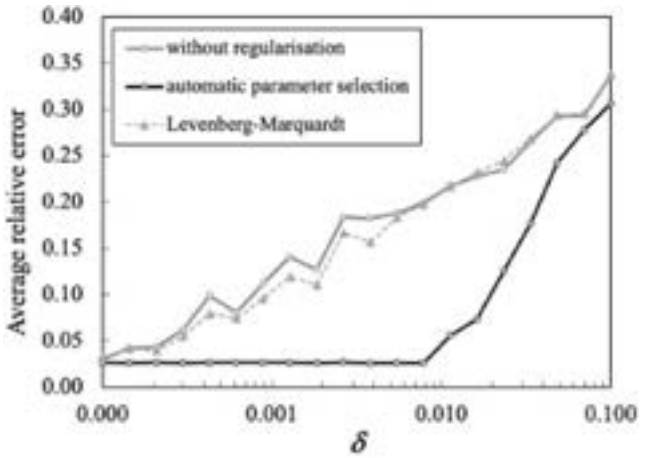

FIGURE 5 | Arch on piers – Average relative error ϵ_δ vs. the noise δ; comparison between the unregularized method, the Levenberg–Marquardt method and the automatic parameter selection with initial estimate $\hat{\mathbf{x}} = (5.0, 2.0 \times 10^3, 5.0, 2.0 \times 10^3)^T$.

Figure 4, the dashed grey line represents the error ϵ_δ calculated using the Levenberg–Marquardt method. The regularizing effects provided by the Levenberg–Marquard approach [53] are not satisfactory in this experiment, where it produces results comparable to our algorithm without regularization.

Figure 5 is analogous to Figure 4, but here the error ϵ_δ is calculated as the average of ϵ_λ over the 100 optimal values of λ (average relative error). For this alternative definition of ϵ_δ, the effect of the regularization is evident: For noise levels below 0.8%, ϵ_δ is approximately 2.6%, whereas, without regularization, it reaches 20%. The Levenberg–Marquardt method performs better than our algorithm without regularization, but its results remain inferior to those obtained using the proposed approach with automatic regularization.

A Levenberg–Marquardt scheme incorporating built-in regularization could potentially achieve results on par with the method

10970207, 2025, 17, Downloaded from https://onlinelibrary.wiley.com/doi/10.1002/nme.70113 by CNR Pisa, Wiley Online Library on [04/09/2025]. See the Terms and Conditions (https://onlinelibrary.wiley.com/terms-and-conditions) on Wiley Online Library for rules of use; OA articles are governed by the applicable Creative Commons License

proposed here; some preliminary ideas in this direction are discussed in [52]. Nevertheless, our approach maintains the advantage of relying on a local trust-region model, which proves effective across a broader range of parameters and thus requires fewer function evaluations, as previously demonstrated in [39]. In support of this, we observed in our experiments that the number of function evaluations for the Levenberg–Marquardt method ranged from two to approximately twenty times that required by the proposed approach.

3.2 | Domed Temple

Let us consider the domed temple depicted in Figure 6. The structure is made up of four 14-meter-high pillars and an octagonal-shaped cloister vault five meters high, resting on a drum inscribed on a 10×11 meters rectangle. The FE model of the structure has 31,052 8-node brick elements and 41,245 nodes [36].

The four constituent materials are shown in Figure 6: Material 1 (red) for the vault, 2 (cyan) for the upper part of the drum, 3 (green) for the lower part of the drum, and 4 (grey) for the pillars. Their mechanical properties are

$$E_1^e = 3.0 \text{ GPa}, \quad \rho_1^e = 1800 \ \frac{\text{kg}}{\text{m}^3}$$
$$E_2^e = 4.0 \text{ GPa}, \quad \rho_2^e = 2000 \ \frac{\text{kg}}{\text{m}^3} \tag{40}$$

$$E_3^e = 3.500 \text{ GPa} \quad \rho_3^e = 1900 \ \frac{\text{kg}}{\text{m}^3}$$
$$E_4^e = 5.0 \text{ GPa} \quad \rho_4^e = 2200 \ \frac{\text{kg}}{\text{m}^3} \tag{41}$$

$$\nu_j^e = 0.25, \quad j = 1, \ldots, 4 \tag{42}$$

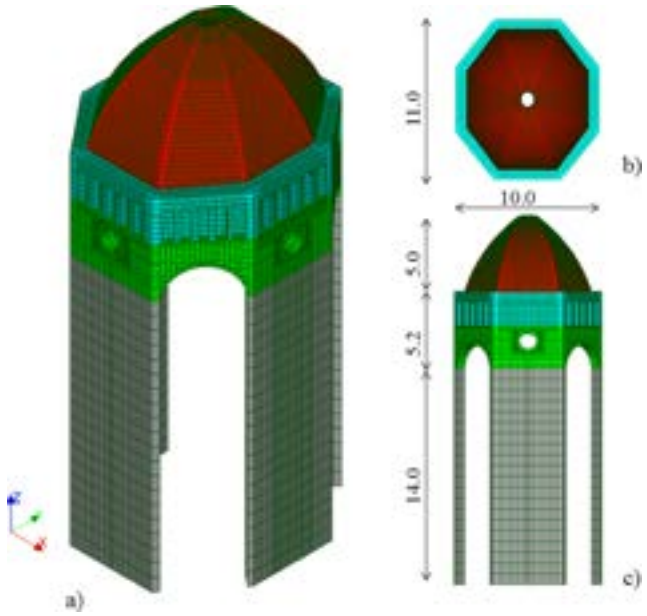

FIGURE 6 | Domed temple. Different colors represent different materials.

The corresponding first ten frequencies (expressed in Hz) are

$$\mathbf{f} = (2.19, 2.23, 3.76, 3.83, 4.32, 4.60, 4.72, 8.26, 8.30, 9.21)^T \tag{43}$$

As done for the arch on piers, we used $\mathbf{f}$ to calculate the optimal value of the parameters vector $\mathbf{x} = (E_1, \rho_1, E_2, \rho_2, E_3, E_4, \rho_4)^T$, which minimizes the objective function (19), assuming that ρ_3 and ν_j are fixed and $\mathbf{x}$ belongs to the box Ω

$$2.0 \le E_1, E_2, E_3, E_4 \le 6.0, \quad 1.6 \times 10^3 \le \rho_1, \rho_2, \rho_4 \le 2.4 \times 10^3 \tag{44}$$

This example is particularly challenging because material 3 weakly affects the frequencies [40]. Such weak dependency implies the ill-conditioning of the inverse problem and small changes in the frequencies will cause significant changes in the optimal material parameters.

As in the case of the arch on piers, for a fixed level of noise δ and a fixed value of the regularization parameter λ, we have calculated the minimum point $\mathbf{x'}_\lambda \in \Omega$ of the objective function (19), where the perturbed frequencies f_i', $i = 1, \ldots, 10$, are calculated according to Equation (27). The initial estimate of $\hat{\mathbf{x}}$ is the middle point of Ω

$$\hat{\mathbf{x}} = (4.0, 2.0 \times 10^3, 4.0, 2.0 \times 10^3, 4.0, 4.0, 2.0 \times 10^3)^T \tag{45}$$

and the maximum relative error of $\hat{\mathbf{x}}$ with respect to the parameter vector

$$\mathbf{x}_0^f = (3.0, 1.8 \times 10^3, 4.0, 2.0 \times 10^3, 3.5, 5.0, 2.2 \times 10^3)^T \tag{46}$$

is $\hat{\epsilon} = 33.3\%$.

The results of the minimization are reported in Figure 7, which shows the plots of the maximum relative error ϵ_λ defined in Equation (28) as a function of the regularization parameter λ, for three values of the relative noise δ added to the frequencies. We emphasize that the value of the regularization parameter λ that minimizes the maximum relative error ϵ_λ depends on the noise level. In particular, as the noise level δ increases, the optimal

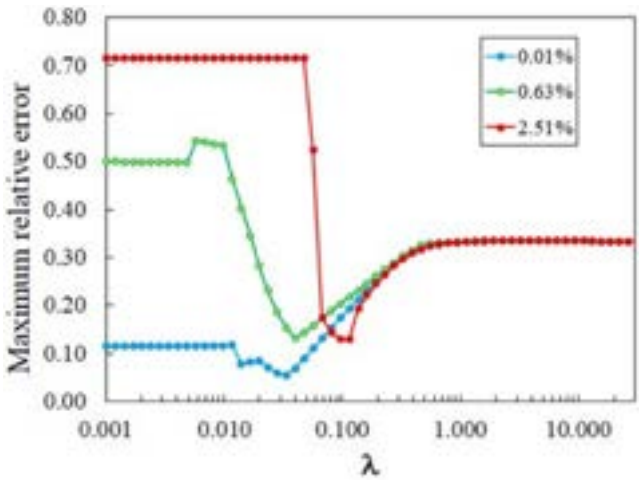

FIGURE 7 | Domed temple – Maximum relative error ϵ_λ for different noise levels δ, vs. the regularization parameter λ and initial estimate $\hat{\mathbf{x}} = (4.0, 2.0 \times 10^3, 4.0, 2.0 \times 10^3, 4.0, 4.0, 2.0 \times 10^3)^T$.

10970207, 2025, 17, Downloaded from https://onlinelibrary.wiley.com/doi/10.1002/nme.70113 by CNR Pisa, Wiley Online Library on [04/09/2025]. See the Terms and Conditions (https://onlinelibrary.wiley.com/terms-and-conditions) on Wiley Online Library for rules of use; OA articles are governed by the applicable Creative Commons License

parameter λ also increases. This behavior is not unexpected and can be understood by looking at (24): As the noise level increases, larger singular values provide non-negligible perturbations in the output, and therefore, it is necessary to apply a more aggressive filtering strategy by increasing the value of the parameter λ.

With reference to Figure 7, for $\delta = 2.51\%$, the optimal value of the regularization parameter is $\lambda = 0.114636$ and the minimum point of the objective function (19) is

$$\mathbf{x}'_\lambda = (3.39, 1.71 \times 10^3, 3.89, 2.0 \times 10^3, 3.93, 5.07, 2.24 \times 10^3)^T \quad (47)$$

with a maximum relative error of $\epsilon_\lambda = 12.9\%$. For $\delta = 0.63\%$, the optimal value of the parameter is $\lambda = 0.039966$ and the minimum point is

$$\mathbf{x}'_\lambda = (3.39, 1.76 \times 10^3, 4.42, 2.13 \times 10^3, 3.96, 4.97, 2.24 \times 10^3)^T \quad (48)$$

with a maximum relative error $\epsilon_\lambda = 13.2\%$. Finally, for $\delta = 0.01\%$, the optimal value of the regularization parameter is $\lambda = 0.033529$ and the minimum point is

$$\mathbf{x}'_\lambda = (3.16, 1.86 \times 10^3, 4.13, 2.10 \times 10^3, 3.68, 5.13, 2.26 \times 10^3)^T \quad (49)$$

with $\epsilon_\lambda = 5.44\%$.

We point out that, even in the absence of noise in the frequencies, introducing a regularization parameter and minimizing the function (19) instead of (18) makes it possible to reduce the maximum relative error ϵ_λ for suitable values of λ, as shown in Figure 7 (blue line).

Figure 8 reports the results of applying the automatic selection of the regularization parameter to the domed temple. With (black line) and without (grey line) regularization, when the noise level approaches 10%, the error ϵ_δ exceeds 50%. The regularization introduces a slightly larger error when there is no noise, but it is much more resistant to noise in the data. In the case of regularization, for values of δ less than 1.13%, the error ϵ_δ remains below 17.2%, unlike the case without regularization, in which ϵ_δ exceeds 48.0%.

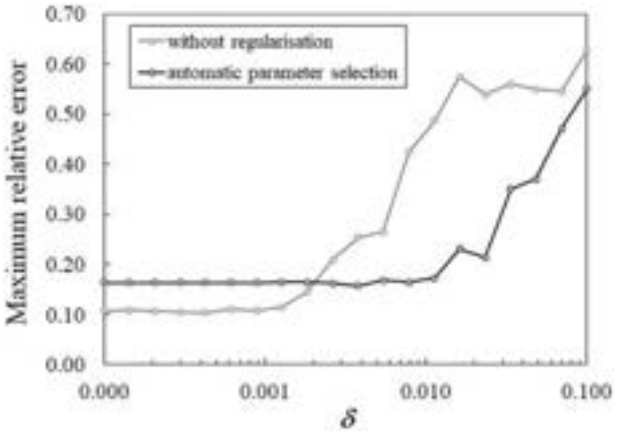

FIGURE 8 | Domed temple – Maximum relative error ϵ_δ vs. the noise δ; comparison between the unregularized method and the automatic parameter selection with the initial estimate $\hat{\mathbf{x}} = (4.0, 2.0 \times 10^3, 4.0, 2.0 \times 10^3, 4.0, 4.0, 2.0 \times 10^3)^T$.

3.3 | The Matilde Donjon in Livorno (Italy)

The Matilde donjon, shown in Figure 9 (left), is a fortified keep belonging to the Fortezza Vecchia (Old Fortress) near the ancient Medici Port of Livorno (Italy). Information about its geometry and the mechanical properties of the constituent materials is provided in [54] and [40]. In October 2017, an ambient vibration monitoring experiment was carried out on the tower (Figure 9, right) in collaboration with the Seismic Observatory of Arezzo (INGV). The ambient vibrations were monitored for a few hours via SARA SS20 seismometric stations arranged in different layouts with a sampling rate of 100 Hz. Six natural frequencies and mode shapes were identified by using the Stochastic Subspace Identification covariance-driven method (SSI–cov) [55] implemented in the MACEC software [56]. The resulting experimental frequencies (expressed in Hz) are

$$\mathbf{f} = (2.68, 3.37, 6.21, 8.10, 10.04, 11.95)^T \quad (50)$$

The FE mesh of the tower shown in Figure 10 consists of 52,560 isoparametric 8-node brick elements and 64,380 nodes, for a total of 193,140 degrees of freedom. The model includes the tower, constituted by an inner part (red circular ring) and an outer part (grey circular ring), and a portion of the Fortress's surrounding walls made of different materials denoted by material 1 (the green walls), material 2 (the cyan wall) and material 3 (the blue walls). The bases of the tower and lateral walls are fixed, and the ends of the walls are prevented from moving along the X and Y directions.

A Global Sensitivity Analysis (GSA) has been performed through the SAFE Toolbox [57] linked to NOSA-ITACA to investigate how variations in Young's moduli and mass densities influence the numerical frequencies. The Elementary Effects Test (EET method [58]) is used to evaluate the sensitivity indices, assuming that the nine input parameters (Young's modulus E_t of the tower and mass densities $\rho_{t,i}$ and $\rho_{t,e}$ of the inner and outer portions of the tower, Young's moduli and the mass densities of the materials 1, 2 and 3, denoted by $E_{m,1}$, $\rho_{m,1}$, $E_{m,2}$, $\rho_{m,2}$, $E_{m,3}$, $\rho_{m,3}$) have a uniform probability distribution function, and adopting the Latin Hypercube method [59] as sampling strategy. The global sensitivity analysis (GSA) conducted in [40] and summarized in Figure 11 shows that the elastic moduli of the tower and wall 1 strongly influence the frequency variation compared to the others. In particular, the tower's Young's modulus impacts all frequencies except for the third, which is heavily affected by the modulus $E_{m,1}$.

The numerical procedure described in the previous section, in the absence of regularization, has been used in [40] to estimate the values of Young's modulus E_t of the tower and Young's moduli ($E_{m,j}$, $j = 1, 2, 3$) of the masonry constituting the Fortress walls, with $\mathbf{x} = (E_t, E_{m,1}, E_{m,2}, E_{m,3})^T$ belonging to the set Ω defined by the following inequalities

$$1.0 \le E_t \le 5.0, \quad 1.0 \le E_{m,j} \le 6.0, \quad j = 1, 2, 3 \quad (51)$$

with Young's moduli expressed in GPa. The Poisson's ratio of masonry is fixed at 0.2, the mass density of the tower's walls is fixed at 1800 kg/m^3 and 2000 kg/m^3 for the inner and outer

10970207, 2025, 17, Downloaded from https://onlinelibrary.wiley.com/doi/10.1002/nme.70113 by CNR Pisa, Wiley Online Library on [04/09/2025]. See the Terms and Conditions (https://onlinelibrary.wiley.com/terms-and-conditions) on Wiley Online Library for rules of use; OA articles are governed by the applicable Creative Commons License

FIGURE 9 | The Matilde donjon (left) and the seismic station on the roof terrace in October 2017 (right).

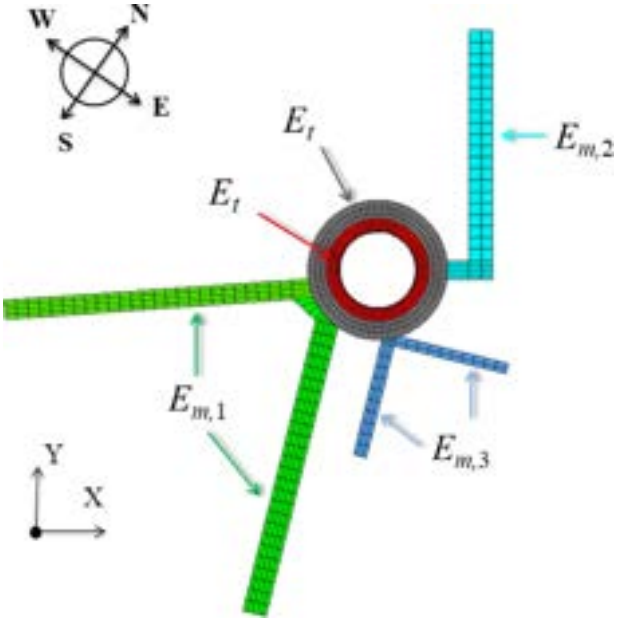

FIGURE 10 | Matilde donjon – FE discretization of the donjon and Fortress walls.

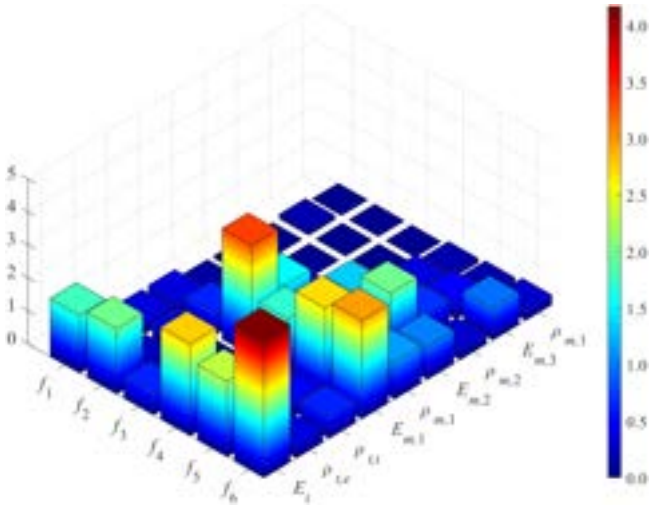

FIGURE 11 | Matilde donjon – EET sensitivity indices for the first six frequencies and nine parameters.

layers, respectively, and the mass density of the side walls is 2000 kg/m^3.

The optimal parameter vector obtained in the absence of noise ($\delta = 0$) and without regularization ($\lambda = 0$, objective function (18)) is

$$\mathbf{x}_0^f = (2.152, 5.808, 5.532, 2.095)^T \tag{52}$$

As pointed out in [40] and confirmed by the sensitivity analysis, the reliability of E_t and $E_{m,1}$ is guaranteed. At the same time, the properties of the materials constituting the remaining walls are marked by uncertainty. The values obtained can be considered acceptable as the most significant uncertainty affects a part of the structure, the right sidewall, whose geometric characteristics (thickness, height, composition), connection degree with the tower, and dynamic properties are unknown. Regardless, the optimal parameter values obtained can describe the global dynamic behavior of the tower.

Table 1 summarizes the numerical frequencies f_i^M of the tower corresponding to the optimal parameter vector in Equation (52) and their relative errors $|\Delta_i|$ with respect to the experimental counterparts f_i, for $i = 1, \ldots, 6$; $|\Delta_i|$ varies between 2% and 3%, except for the third and sixth frequencies.

Figure 12 reports the regularization results. The objective function (19) has been minimized in the set Ω defined in Equation (51)

10970207, 2025, 17, Downloaded from https://onlinelibrary.wiley.com/doi/10.1002/nme.70113 by CNR Pisa, Wiley Online Library on [04/09/2025]. See the Terms and Conditions (https://onlinelibrary.wiley.com/terms-and-conditions) on Wiley Online Library for rules of use; OA articles are governed by the applicable Creative Commons License

TABLE 1 | Matilde donjon – Experimental frequencies $\mathbf{f}$ and numerical frequencies $\mathbf{f}^M$ calculated at the optimal parameter vector $\mathbf{x}_0^f$.

	f_i [Hz]	f_i^M [Hz]	$\lvert\Delta_i\rvert$ [%]
Mode 1	2.68	2.76	2.99
Mode 2	3.37	3.33	1.20
Mode 3	6.21	6.51	4.83
Mode 4	8.10	7.90	2.47
Mode 5	10.04	9.81	2.29
Mode 6	11.95	11.10	7.11

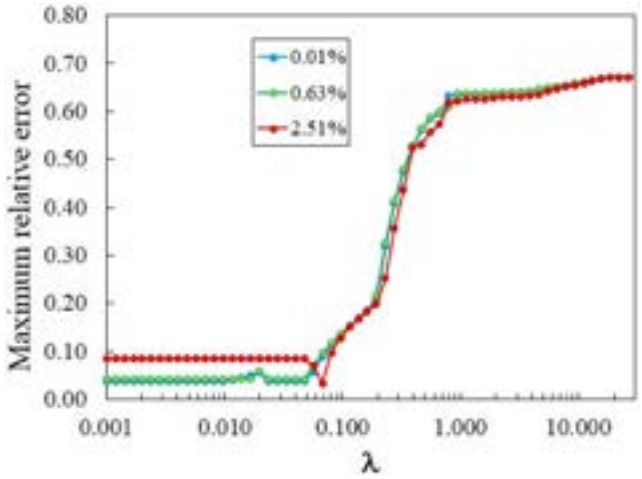

FIGURE 12 | Matilde donjon (six experimental frequencies and four unknown parameters) – Maximum relative error ϵ_λ for different noise levels δ, vs. the regularization parameter λ and initial estimate $\widehat{\mathbf{x}} = (3.0, 3.5, 3.5, 3.5)^T$.

using the experimental frequencies (50) perturbed according to (27). Figure 12 shows the maximum relative error ϵ_λ for different noise levels δ versus the regularization parameter λ. The initial estimate $\widehat{\mathbf{x}} = (3.0, 3.5, 3.5, 3.5)^T$ coincides with the middle point of Ω, whose corresponding maximum relative error is $\widehat{\epsilon} = 67\%$. Figure 12 shows that the noise δ does not affect the model updating solution; for $\delta = 2.51\%$, the choice of $\lambda = 0.06769$ reduces the error ϵ_λ from about 10% to 5.0%, the same value obtained for zero or very low noise levels.

For this problem, the noise does not significantly impact the quality of the solution. The knowledge of 6 frequencies already determines the underlying parameters with good accuracy.

The situation is different when 5 parameters and 5 frequencies are considered. In this new formulation of the problem, the goal is to estimate the values of Young's modulus E_t and mass density ρ_t of the inner and outer layers ($\rho_{t,i} = \rho_{t,e} = \rho_t$) of the tower's walls and Young's moduli $E_{m,1}$, $E_{m,2}$ and $E_{m,3}$ of the masonry constituting the Fortress walls, with $\mathbf{x} = (E_t, \rho_t, E_{m,1}, E_{m,2}, E_{m,3})^T$. belonging to the set Ω defined by

$$1.0 \le E_t \le 5.0, \quad 1700 \le \rho_t \le 2100, \quad 1.0 \le E_{m,j} \le 6.0, \quad j = 1, 2, 3 \tag{53}$$

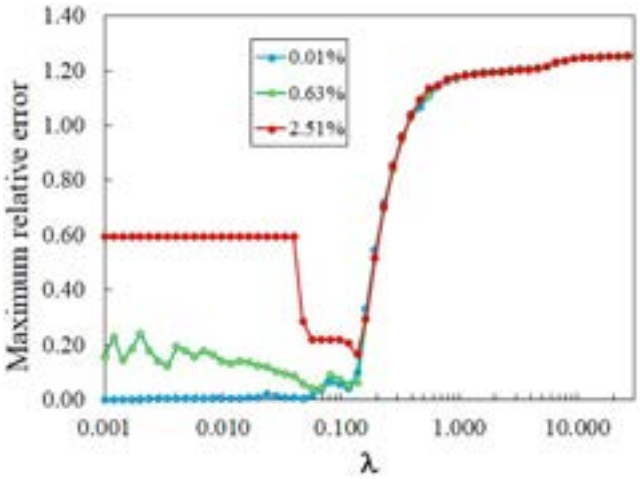

FIGURE 13 | Matilde donjon (five experimental frequencies and five unknown parameters) – Maximum relative error ϵ_λ for different noise levels δ, vs. the regularization parameter λ and initial estimate $\widehat{\mathbf{x}} = (3.0, 1900.0, 3.5, 3.5, 3.5)^T$.

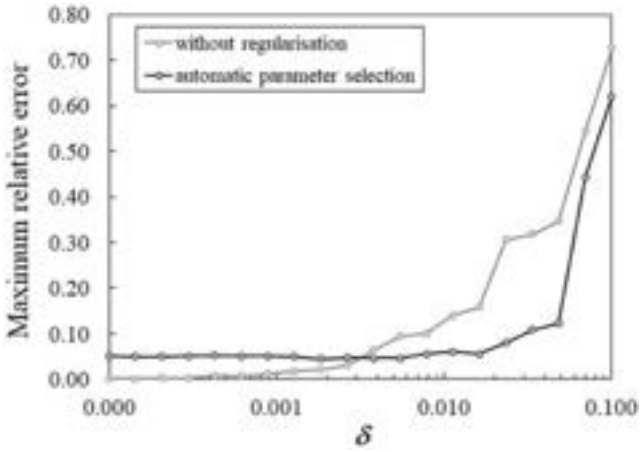

FIGURE 14 | Matilde donjon – Maximum relative error ϵ_δ vs. the noise δ; comparison between the unregularized method and the automatic parameter selection with the initial estimate $\widehat{\mathbf{x}} = (3.0, 1900.0, 3.5, 3.5, 3.5)^T$.

The Poisson's ratio of masonry is fixed at 0.2 and the mass density of the side walls is 2000 kg/m^3.

The optimal parameters vector obtained in the absence of noise ($\delta = 0$) and without regularization ($\lambda = 0$, objective function (18)) is

$$\mathbf{x}_0^f = (2.336, 2.069 \times 10^3, 5.782, 3.773, 1.549)^T \tag{54}$$

Figures 13 and 14 report the regularization results. The objective function (19) has been minimized in the set Ω defined in Equation (53) using the first five experimental frequencies in Equation (50) perturbed according to (27). The initial estimate $\widehat{\mathbf{x}} = (3.0, 1900.0, 3.5, 3.5, 3.5)^T$ coincides with the middle point of Ω and $\widehat{\epsilon} = 126.0\%$. Figure 13 shows the maximum relative error ϵ_λ for different noise levels δ vs. the regularization parameter λ. For $\delta = 2.51\%$, the optimal value of the regularization parameter

10970207, 2025, 17, Downloaded from https://onlinelibrary.wiley.com/doi/10.1002/nme.70113 by CNR Pisa, Wiley Online Library on [04/09/2025]. See the Terms and Conditions (https://onlinelibrary.wiley.com/terms-and-conditions) on Wiley Online Library for rules of use; OA articles are governed by the applicable Creative Commons License

is $\lambda = 0.136645$ and the minimum point of the objective function (19) is

$$\mathbf{x}_\lambda = (1.946, 1.80 \times 10^3, 5.598, 3.762, 1.622)^T \tag{55}$$

with a maximum relative error $\epsilon_\lambda = 16.5\%$. For $\delta = 0.63\%$, the optimal value of the parameter is $\lambda = 0.056785$ and the minimum point is

$$\mathbf{x}_\lambda = (2.265, 2.15 \times 10^3, 5.704, 3.917, 1.549)^T \tag{56}$$

with a maximum relative error $\epsilon_\lambda = 4\%$. Finally, for $\delta = 0.01\%$, the optimal value of the regularization parameter, the minimum point, and the corresponding ϵ_λ coincide with those calculated without noise ($\delta = 0.0$).

Figure 14 reports the results of applying the automatic selection of the regularization parameter. With (black line) and without (grey line) regularization, when the noise level approaches 10%, the error ϵ_δ exceeds 60%. The regularization introduces a slightly larger error when there is no noise, but it is much more resistant to noise in the data. In the case of regularization, for values of δ less than 2.3%, the error ϵ_δ remains below 8.0%, unlike the case without regularization, in which ϵ_δ exceeds 30.0%.

4 | Conclusions

This article investigates the effects of regularization on the model updating of engineering structures. The goal is to develop a robust method able to overcome the well-known drawbacks affecting inverse problems, like ill-posedness and the consequent possible significant changes in the solution (the unknown mechanical properties) due to minimal input perturbation (the experimental frequencies).

We present a strategy for choosing a regularization parameter for the trust-region approach based on Lanczos projections for model updating in structural applications developed by the Authors and implemented in the finite element code NOSA-ITACA.

Whenever information on the noise level in the input data is available, the method can be used to select the regularization parameter appropriately; a theoretical justification for this choice is given using the Tikhonov regularization framework. An automatic parameter selection procedure has been developed when this information is unavailable. This procedure analyzes the condition number of the least squares problem by looking at the Jacobian and selects a regularization parameter that filters the largest possible noise level without introducing significant changes in the problem. The details needed for a reliable implementation that works well with the trust-region scheme have been discussed, such as proper scaling of the parameters and a relaxation procedure for updating the regularization parameter.

The automatic procedure has been tested on some non-trivial examples where artificial noise has been added to the frequencies and verified to be very effective.

Acknowledgments

This research has been partially supported by the Italian National Research Council (REVOLUTION Project, Progetti di Ricerca @CNR, 2022–2025). The work of Leonardo Robol has been supported by the National Research Center in High Performance Computing, Big Data and Quantum Computing (CN1 – Spoke 6), by the Italian Ministry of University and Research awarded to the Department of Mathematics, University of Pisa, CUP I57G22000700001. These supports are gratefully acknowledged. Open access publishing facilitated by Consiglio Nazionale delle Ricerche, as part of the Wiley - CRUI-CARE agreement.

Data Availability Statement

The data that support the findings of this study are available from the corresponding author upon reasonable request.

References

1. J. E. Mottershead and M. I. Friswell, "Model Updating in Structural Dynamics: A Survey," *Journal of Sound and Vibration* 167, no. 2 (1993): 347–375.

2. M. I. Friswell and J. E. Mottershead, *Finite Element Model Updating in Structural Dynamics*, vol. 38 (Springer Science & Business Media, 1995).

3. V. Compan, P. Pachon, M. Camara, P. B. Lourenco, and A. Saez, "Structural Safety Assessment of Geometrically Complex Masonry Vaults by Nonlinear Analysis. The Chapel of the Würzburg Residence (Germany)," *Engineering Structures* 40 (2017): 1–13.

4. A. Bautista-De Castro, L. J. Sanchez-Aparicio, L. F. Ramos, J. Sena-Cruz, and D. Gonzalez-Aguilera, "Integrating Geomatic Approaches, Operational Modal Analysis, Advanced Numerical and Updating Methods to Evaluate the Current Safety Conditions of the Historical Bôco Bridge," *Construction and Building Materials* 158 (2018): 961–984.

5. A. C. Altunisik, F. Y. Okur, A. Fuat Genç, M. Günaydin, and S. Adanur, "Automated Model Updating of Historical Masonry Structures Based on Ambient Vibration Measurements," *Journal of Performance of Constructed Facilities* 32, no. 1 (2018): 04017126.

6. E. Bassoli, L. Vincenzi, A. M. D'Altri, S. de Miranda, M. Forghieri, and G. Castellazzi, "Ambient Vibration-Based Finite Element Model Updating of an Earthquake-Damaged Masonry Tower," *Structural Control and Health Monitoring* 25, no. 5 (2018): e2150.

7. R. Ferrari, D. Froio, E. Rizzi, C. Gentile, and E. N. Chatzi, "Model Updating of a Historic Concrete Bridge by Sensitivity and Global Optimisation-Based Latin Hypercube Sampling," *Engineering Structures* 179 (2019): 139–160.

8. G. Dessena, D. I. Ignatyev, J. F. Whidborne, and L. Z. Fragonara, "A Global–Local Meta-Modelling Technique for Model Updating," *Computer Methods in Applied Mechanics and Engineering* 418 (2024): 116511.

9. P. C. Hansen, "Regularization Tools: A Matlab Package for Analysis and Solution of Discrete Ill-Posed Problems," *Numerical Algorithms* 6, no. 1 (1994): 1–35.

10. P. C. Hansen, *Rank-Deficient and Discrete Ill-Posed Problems* (SIAM, 1998).

11. P. C. Hansen, *Discrete Inverse Problems: Insight and Algorithms* (SIAM series on Fundamentals of Algorithms, 2010).

12. A. N. Tikhonov, A. V. Goncharsky, V. V. Stepanov, and A. G. Yagola, *Numerical Methods for the Solution of Ill-Posed Problems*, vol. 328 (Springer Science & Business Media, 2013).

13. S. Noschese and L. Reichel, "Some Matrix Nearness Problems Suggested by Tikhonov Regularisation," *Linear Algebra and its Applications* 502 (2016): 366–386.

14. H. Ahmadian, J. E. Mottershead, and M. I. Friswell, "Regularisation Methods for Finite Element Model Updating," *Mechanical Systems and Signal Processing* 12, no. 1 (1998): 47–64.

10970207, 2025, 17, Downloaded from https://onlinelibrary.wiley.com/doi/10.1002/nme.70113 by CNR Pisa, Wiley Online Library on [04/09/2025]. See the Terms and Conditions (https://onlinelibrary.wiley.com/terms-and-conditions) on Wiley Online Library for rules of use; OA articles are governed by the applicable Creative Commons License

15. C. Mares, M. I. Friswell, and J. E. Mottershead, "Model Updating Using Robust Estimation," *Mechanical Systems and Signal Processing* 16, no. 1 (2002): 169–183.

16. P. G. Bakir, E. Reynders, and G. De Roeck, "Sensitivity-Based Finite Element Model Updating Using Constrained Optimisation With a Trust Region Algorithm," *Journal of Sound and Vibration* 305, no. 1-2 (2007): 211–225.

17. B. Titurus and M. I. Friswell, "Regularisation in Model Updating," *International Journal for Numerical Methods in Engineering* 75, no. 4 (2008): 440–478.

18. J. E. Mottershead, M. Link, and M. I. Friswell, "The Sensitivity Method in Finite Element Model Updating: A Tutorial," *Mechanical Systems and Signal Processing* 25, no. 7 (2011): 2275–2296.

19. A. De Falco, M. Girardi, D. Pellegrini, L. Robol, and G. Sevieri, "Model Parameter Estimation Using Bayesian and Deterministic Approaches: The Case Study of the Maddalena Bridge," *Procedia Structural Integrity* 11 (2018): 210–217.

20. S. Wang, M. Xu, Z. Xia, and Y. Li, "A Novel Tikhonov Regularisation-Based Iterative Method for Structural Damage Identification of Offshore Platforms," *Journal of Marine Science and Technology* 24 (2019): 575–592.

21. P. Reumers, M. Schevenels, and G. Lombaert, "Density Filtering Regularisation of Finite Element Model Updating Problems," *Mechanical Systems and Signal Processing* 128 (2019): 282–294.

22. M. Mazzotti, Q. Mao, I. Bartoli, and S. Livadiotis, "A Multiplicative Regularised Gauss-Newton Method With Trust Region Sequential Quadratic Programming for Structural Model Updating," *Mechanical Systems and Signal Processing* 131 (2019): 417–433.

23. M. Rezaiee-Pajand, H. Sarmadi, and A. Entezami, "A Hybrid Sensitivity Function and Lanczos Bidiagonalization-Tikhonov Method for Structural Model Updating: Application to a Full-Scale Bridge Structure," *Applied Mathematical Modelling* 89 (2021): 860–884.

24. J. L. Beck and L. S. Katafygiotis, "Updating Models and Their Uncertainties. I: Bayesian Statistical Framework," *Journal of Engineering Mechanics* 124, no. 4 (1998): 455–461.

25. L. S. Katafygiotis and J. L. Beck, "Updating Models and Their Uncertainties. II: Model Identifiability," *Journal of Engineering Mechanics* 124, no. 4 (1998): 463–467.

26. M. W. Vanick, J. L. Beck, and S. K. Au, "Bayesian Probabilistic Approach to Structural Health Monitoring," *Journal of Engineering Mechanics* 126 (2000): 738–745.

27. C. Mares, J. E. Mottershead, and M. I. Friswell, "Stochastic Model Updating: Part 1 - Theory and Simulated Example," *Mechanical Systems and Signal Processing* 20, no. 7 (2006): 1674–1695.

28. D. Calvetti and E. Somersalo, *Introduction to Bayesian Scientific Computing* (Springer, 2007).

29. E. Simoen, G. De Roeck, and G. Lombaert, "Dealing With Uncertainty in Model Updating for Damage Assessment: A Review," *Mechanical Systems and Signal Processing* 56 (2015): 123–149.

30. D. Calvetti and E. Somersalo, "Inverse Problems: From Regularisation to Bayesian Inference," *Wiley Interdisciplinary Reviews: Computational Statistics* 10, no. 3 (2018): e1427.

31. S. Monchetti, C. Viscardi, M. Betti, and G. Bartoli, "Bayesian-Based Model Updating Using Natural Frequency Data for Historic Masonry Towers," *Probabilistic Engineering Mechanics* 70 (2022): 103337.

32. S. Monchetti, C. Viscardi, M. Betti, and F. Clementi, "Comparison Between Bayesian Updating and Approximate Bayesian Computation for Model Identification of Masonry Towers Through Dynamic Data," *Bulletin of Earthquake Engineering* 22 (2024): 3491–3509.

33. D. Raviolo, M. Civera, and L. Zanotti Fragonara, "A Bayesian Sampling Optimisation Strategy for Finite Element Model Updating," *Journal of Civil Structural Health Monitoring* 15 (2025): 1585–1607.

34. G. Bolzon, R. Fedele, and G. Maier, "Parameter Identification of a Cohesive Crack Model by Kalman Filter," *Computer Methods in Applied Mechanics and Engineering* 191, no. 25-26 (2002): 2847–2871.

35. M. Girardi, C. Padovani, and D. Pellegrini, "The NOSA-ITACA Code for the Safety Assessment of Ancient Constructions: A Case Study in Livorno," *Advances in Engineering Software* 89 (2015): 64–76.

36. V. Binante, M. Girardi, C. Padovani, et al., "NOSA-ITACA 1.1 documentation, Technical Report ISTI-CNR 2017-SW-013," 2017.

37. M. Girardi, C. Padovani, D. Pellegrini, M. Porcelli, and L. Robol, "Numerical Modelling of Historical Masonry Structures With the Finite Element Code NOSA-ITACA," in *Mathematical Modeling in Cultural Heritage. MACH 2021. Springer INdAM Series*, vol. 55, ed. G. Bretti, C. Cavaterra, M. Solci, and M. Spagnuolo (Springer, 2023), https://doi.org/10.1007/978-981-99-3679-3-9.

38. M. Girardi, C. Padovani, D. Pellegrini, and L. Robol, "Model Updating Procedure to Enhance Structural Analysis in the FE Code NOSA-ITACA," *Journal of Performance of Constructed Facilities* 33, no. 4 (2019): 04019041.

39. M. Girardi, C. Padovani, D. Pellegrini, M. Porcelli, and L. Robol, "Finite Element Model Updating for Structural Applications," *Journal of Computational and Applied Mathematics* 370 (2020): 112675.

40. M. Girardi, C. Padovani, D. Pellegrini, and L. Robol, "A Finite Element Model Updating Method Based on Global Optimisation," *Mechanical Systems and Signal Processing* 152 (2021): 107372.

41. J. Stoer and R. Bulirsch, *Introduction to Numerical Analysis*, 3rd ed. (Springer, 2002).

42. S. Boyd and L. Vandenberghe, *Convex Optimization* (Cambridge University Press, 2004).

43. O. Scherzer, "The Use of Morozov's Discrepancy Principle for Tikhonov Regularisation for Solving Nonlinear Ill-Posed Problems," *Computing* 51, no. 1 (1993): 45–60, https://doi.org/10.1007/BF02243828.

44. C. G. Farquharson and D. W. Oldenburg, "A Comparison of Automatic Techniques for Estimating the Regularisation Parameter in Non–Linear Inverse Problems," *Geophysical Journal International* 156, no. 3 (2004): 411–425, https://doi.org/10.1111/j.1365-246X.2004.02190.x.

45. B. Weber, P. Paultre, and J. Proulx, "Consistent Regularisation of Nonlinear Model Updating for Damage Identification," *Mechanical Systems and Signal Processing* 23, no. 6 (2009): 965–1985, https://doi.org/10.1016/j.ymssp.2008.04.011.

46. G. H. Golub, M. Heath, and G. Wahba, "Generalised Cross Validation as a Method for Choosing a Good Ridge Parameter," *Technometrics* 21, no. 2 (1979): 215–223.

47. B. Weber, P. Paultre, and J. Proulx, "Structural Damage Detection Using Nonlinear Parameter Identification With Tikhonov Regularisation," *Structural Control and Health Monitoring* 14, no. 3 (2007): 406–427, https://doi.org/10.1002/stc.164.

48. C. Faure, F. Ablitzer, J. Antoni, and C. Pézerat, "Empirical and Fully Bayesian Approaches for the Identification of Vibration Sources From Transverse Displacement Measurements," *Mechanical Systems and Signal Processing* 94 (2017): 180–201, https://doi.org/10.1016/j.ymssp.2017.02.023.

49. P. Hansen and D. O'Leary, "The Use of the L–Curve in the Regularisation of Discrete Ill–Posed Problems," *SIAM Journal on Scientific Computing* 14, no. 6 (1993): 1487–1503, https://doi.org/10.1137/0914086.

50. X. Hua, Y. Ni, and J. Ko, "Adaptive Regularisation Parameter Optimisation in Output–Error–Based Finite Element Model Updating," *Mechanical Systems and Signal Processing* 23, no. 3 (2009): 563–579, https://doi.org/10.1016/j.ymssp.2008.05.002.

10970207, 2025, 17, Downloaded from https://onlinelibrary.wiley.com/doi/10.1002/nme.70113 by CNR Pisa, Wiley Online Library on [04/09/2025]. See the Terms and Conditions (https://onlinelibrary.wiley.com/terms-and-conditions) on Wiley Online Library for rules of use; OA articles are governed by the applicable Creative Commons License

51. X. Li and S. Law, "Adaptive Tikhonov Regularisation for Damage Detection Based on Nonlinear Model Updating," *Mechanical Systems and Signal Processing* 24, no. 6 (2010): 1646–1664, https://doi.org/10.1016/j.ymssp.2010.02.006.

52. S. Bellavia, B. Morini, and E. Riccietti, "On an Adaptive Regularization for Ill-Posed Nonlinear Systems and Its Trust-Region Implementation," *Computational Optimization and Applications* 64 (2016): 1–30.

53. M. Hanke, "A Regularizing Levenberg-Marquardt Scheme With Applications to Inverse Groundwater Filtration Problems," *Inverse Problems* 13, no. 1 (1997): 79.

54. P. Barsocchi, G. Bartoli, M. Betti, et al., "Wireless Sensor Networks for Continuous Structural Health Monitoring of Historic Masonry Towers," *International Journal of Architectural Heritage* 15, no. 1 (2020): 22–44.

55. B. Peeters and G. De Roeck, "Reference-Based Stochastic Subspace Identification for Output-Only Modal Analysis," *Mechanical Systems and Signal Processing* 13, no. 6 (1999): 855–878.

56. E. Reynders, M. Schevenels, and G. De Roeck, "Macec 3.3: A Matlab toolbox for experimental and operational modal analysis-user manual," 2014.

57. F. Pianosi, F. Sarrazin, and T. Wagener, "A Matlab Toolbox for Global Sensitivity Analysis," *Environmental Modelling and Software* 70 (2015): 80–85.

58. M. D. Morris, "Factorial Sampling Plans for Preliminary Computational Experiments," *Technometrics* 33, no. 2 (1991): 161–174.

59. M. D. McKay, R. J. Beckman, and W. J. Conover, "Comparison of Three Methods for Selecting Values of Input Variables in the Analysis of Output From a Computer Code," *Technometrics* 21, no. 2 (1979): 239–245.

10970207, 2025, 17, Downloaded from https://onlinelibrary.wiley.com/doi/10.1002/nme.70113 by CNR Pisa, Wiley Online Library on [04/09/2025]. See the Terms and Conditions (https://onlinelibrary.wiley.com/terms-and-conditions) on Wiley Online Library for rules of use; OA articles are governed by the applicable Creative Commons License